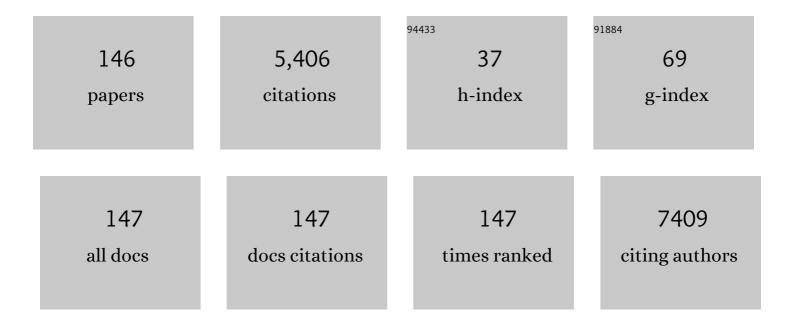
List of Publications by Year in descending order

Source: https://exaly.com/author-pdf/6409649/publications.pdf

Version: 2024-02-01



\{/FN_\{/F1\}/11

#	Article	IF	CITATIONS
1	High Mobility MoS ₂ Transistor with Low Schottky Barrier Contact by Using Atomic Thick hâ€BN as a Tunneling Layer. Advanced Materials, 2016, 28, 8302-8308.	21.0	398
2	Observation of Atomic Diffusion at Twin-Modified Grain Boundaries in Copper. Science, 2008, 321, 1066-1069.	12.6	352
3	Dynamic Evolution of Conducting Nanofilament in Resistive Switching Memories. Nano Letters, 2013, 13, 3671-3677.	9.1	327
4	Interface Engineering for Highâ€Performance Topâ€Gated MoS ₂ Fieldâ€Effect Transistors. Advanced Materials, 2014, 26, 6255-6261.	21.0	272
5	Switching Kinetic of VCMâ€Based Memristor: Evolution and Positioning of Nanofilament. Advanced Materials, 2015, 27, 5028-5033.	21.0	176
6	Flexible ferroelectric element based on van der Waals heteroepitaxy. Science Advances, 2017, 3, e1700121.	10.3	174
7	Single Crystalline PtSi Nanowires, PtSi/Si/PtSi Nanowire Heterostructures, and Nanodevices. Nano Letters, 2008, 8, 913-918.	9.1	166
8	Thermal Stability and Performance of NbSiTaTiZr High-Entropy Alloy Barrier for Copper Metallization. Journal of the Electrochemical Society, 2011, 158, H1161.	2.9	166
9	In situ Control of Atomic-Scale Si Layer with Huge Strain in the Nanoheterostructure NiSi/Si/NiSi through Point Contact Reaction. Nano Letters, 2007, 7, 2389-2394.	9.1	136
10	Van der Waals heteroepitaxial AZO/NiO/AZO/muscovite (ANA/muscovite) transparent flexible memristor. Nano Energy, 2019, 56, 322-329.	16.0	125
11	Well-aligned ZnOnanowires with excellent field emission and photocatalytic properties. Nanoscale, 2012, 4, 1471-1475.	5.6	107
12	In-situ TEM Observation of Repeating Events of Nucleation in Epitaxial Growth of Nano CoSi ₂ in Nanowires of Si. Nano Letters, 2008, 8, 2194-2199.	9.1	94
13	Facile synthesis of mesoporous NiFe 2 O 4 /CNTs nanocomposite cathode material for high performance asymmetric pseudocapacitors. Applied Surface Science, 2018, 433, 1100-1112.	6.1	92
14	Direct Observation of Dualâ€Filament Switching Behaviors in Ta ₂ O ₅ â€Based Memristors. Small, 2017, 13, 1603116.	10.0	85
15	Oxide Heteroepitaxy for Flexible Optoelectronics. ACS Applied Materials & Interfaces, 2016, 8, 32401-32407.	8.0	81
16	Rational Design of ZnO:H/ZnO Bilayer Structure for High-Performance Thin-Film Transistors. ACS Applied Materials & Interfaces, 2016, 8, 7862-7868.	8.0	76
17	Homogeneous Nucleation of Epitaxial CoSi ₂ and NiSi in Si Nanowires. Nano Letters, 2009, 9, 2337-2342.	9.1	66
18	Dielectric Engineering of a Boron Nitride/Hafnium Oxide Heterostructure for Highâ€Performance 2D Field Effect Transistors. Advanced Materials, 2016, 28, 2062-2069.	21.0	65

#	Article	IF	CITATIONS
19	Phase transformation and thermoelectric properties of bismuth-telluride nanowires. Nanoscale, 2013, 5, 4669.	5.6	63
20	Supercritical CO ₂ â€Assisted SiO <i>_x</i> /Carbon Multi‣ayer Coating on Si Anode for Lithiumâ€Ion Batteries. Advanced Functional Materials, 2021, 31, 2104135.	14.9	59
21	Observation of Resistive Switching Behavior in Crossbar Core–Shell Ni/NiO Nanowires Memristor. Small, 2018, 14, 1703153.	10.0	58
22	Growth of High-Density Titanium Silicide Nanowires in a Single Direction on a Silicon Surface. Nano Letters, 2007, 7, 885-889.	9.1	56
23	Resistive switching of Au/ZnO/Au resistive memory: an in situ observation of conductive bridge formation. Nanoscale Research Letters, 2012, 7, 559.	5.7	53
24	Atomic-scale investigation of Lithiation/Delithiation mechanism in High-entropy spinel oxide with superior electrochemical performance. Chemical Engineering Journal, 2021, 420, 129838.	12.7	53
25	Excellent piezoelectric and electrical properties of lithium-doped ZnO nanowires for nanogenerator applications. Nano Energy, 2014, 8, 291-296.	16.0	48
26	Low Power Consumption Nanofilamentary ECM and VCM Cells in a Single Sidewall of Highâ€Density VRRAM Arrays. Advanced Science, 2019, 6, 1902363.	11.2	47
27	Growth of CulnSe2and In2Se3/CulnSe2Nano-Heterostructures through Solid State Reactions. Nano Letters, 2011, 11, 4348-4351.	9.1	46
28	Measurement of Interlayer Screening Length of Layered Graphene by Plasmonic Nanostructure Resonances. Journal of Physical Chemistry C, 2013, 117, 22211-22217.	3.1	44
29	Revealing Controllable Nanowire Transformation through Cationic Exchange for RRAM Application. Nano Letters, 2014, 14, 2759-2763.	9.1	44
30	Revealing conducting filament evolution in low power and high reliability Fe3O4/Ta2O5 bilayer RRAM. Nano Energy, 2018, 53, 871-879.	16.0	44
31	High on/off ratio black phosphorus based memristor with ultra-thin phosphorus oxide layer. Applied Physics Letters, 2019, 115, .	3.3	42
32	In Situ TEM and Energy Dispersion Spectrometer Analysis of Chemical Composition Change in ZnO Nanowire Resistive Memories. Analytical Chemistry, 2013, 85, 3955-3960.	6.5	41
33	Synthesis and growth mechanism of pentagonal Cu nanobats with field emission characteristics. Nanotechnology, 2006, 17, 719-722.	2.6	40
34	Kinetic Competition Model and Size-Dependent Phase Selection in 1-D Nanostructures. Nano Letters, 2012, 12, 3115-3120.	9.1	40
35	Dynamic Observation of Phase Transformation Behaviors in Indium(III) Selenide Nanowire Based Phase Change Memory. ACS Nano, 2014, 8, 9457-9462.	14.6	39
36	In Situ Study of Spinel Ferrite Nanocrystal Growth Using Liquid Cell Transmission Electron Microscopy. Chemistry of Materials, 2015, 27, 8146-8152.	6.7	39

#	Article	IF	CITATIONS
37	Dynamics of Nanoscale Dendrite Formation in Solution Growth Revealed Through in Situ Liquid Cell Electron Microscopy. Nano Letters, 2018, 18, 6427-6433.	9.1	38
38	Vertically well-aligned epitaxial Ni31Si12 nanowire arrays with excellent field emission properties. Applied Physics Letters, 2008, 93, 113109.	3.3	37
39	Cobalt Silicide Nanostructures: Synthesis, Electron Transport, and Field Emission Properties. Crystal Growth and Design, 2009, 9, 4514-4518.	3.0	36
40	Synthesis and Characterization of One-Dimensional Ag-Doped ZnO/Ga-Doped ZnO Coaxial Nanostructure Diodes. ACS Applied Materials & amp; Interfaces, 2014, 6, 5183-5191.	8.0	35
41	Copper silicide/silicon nanowire heterostructures: in situ TEM observation of growth behaviors and electron transport properties. Nanoscale, 2013, 5, 5086.	5.6	34
42	Observing Growth of Nanostructured ZnO in Liquid. Chemistry of Materials, 2016, 28, 4507-4511.	6.7	34
43	Sub-nA Low-Current HZO Ferroelectric Tunnel Junction for High-Performance and Accurate Deep Learning Acceleration. , 2019, , .		34
44	Probing the electrochemical properties of an electrophoretically deposited Co ₃ O ₄ /rGO/CNTs nanocomposite for supercapacitor applications. RSC Advances, 2016, 6, 60578-60586.	3.6	33
45	In-situ TEM observation of Multilevel Storage Behavior in low power FeRAM device. Nano Energy, 2017, 34, 103-110.	16.0	33
46	Observing topotactic phase transformation and resistive switching behaviors in low power SrCoOx memristor. Nano Energy, 2020, 72, 104683.	16.0	33
47	Polarizationâ€Resolved Broadband MoS ₂ /Black Phosphorus/MoS ₂ Optoelectronic Memory with Ultralong Retention Time and Ultrahigh Switching Ratio. Advanced Functional Materials, 2021, 31, 2100781.	14.9	33
48	Growth of Multiple Metal/Semiconductor Nanoheterostructures through Point and Line Contact Reactions. Nano Letters, 2010, 10, 3984-3989.	9.1	31
49	Facile production of graphene nanosheets comprising nitrogen-doping through in situ cathodic plasma formation during electrochemical exfoliation. Journal of Materials Chemistry C, 2017, 5, 2597-2602.	5.5	31
50	Sandwich-Nanostructured n-Cu ₂ O/AuAg/p-Cu ₂ O Photocathode with Highly Positive Onset Potential for Improved Water Reduction. ACS Applied Materials & Interfaces, 2019, 11, 38625-38632.	8.0	30
51	Taper PbZr _{0.2} Ti _{0.8} O ₃ Nanowire Arrays: From Controlled Growth by Pulsed Laser Deposition to Piezopotential Measurements. ACS Nano, 2012, 6, 2826-2832.	14.6	29
52	Atomicâ€Scale Fabrication of Inâ€Plane Heterojunctions of Few‣ayer MoS ₂ via In Situ Scanning Transmission Electron Microscopy. Small, 2020, 16, e1905516.	10.0	29
53	Phosphorus-Doped p–n Homojunction ZnO Nanowires: Growth Kinetics in Liquid and Their Optoelectronic Properties. Chemistry of Materials, 2015, 27, 4216-4221.	6.7	28
54	In situ atomic scale investigation of Li7La3Zr2O12-based Li+-conducting solid electrolyte during calcination growth. Nano Energy, 2020, 71, 104625.	16.0	28

#	Article	IF	CITATIONS
55	Atomic-Scale Investigation of Electromigration with Different Directions of Electron Flow into High-Density Nanotwinned Copper through In Situ HRTEM. Acta Materialia, 2021, 219, 117250.	7.9	28
56	High-yield synthesis of ZnO nanowire arrays and their opto-electrical properties. Nanoscale, 2012, 4, 1476-1480.	5.6	27
57	A novel high-performance and energy-efficient RRAM device with multi-functional conducting nanofilaments. Nano Energy, 2021, 82, 105717.	16.0	27
58	Direct observation of electromigration-induced surface atomic steps in Cu lines by in situ transmission electron microscopy. Applied Physics Letters, 2007, 90, 203101.	3.3	26
59	Direct observation of melting behaviors at the nanoscale under electron beam and heat to form hollow nanostructures. Nanoscale, 2012, 4, 4702.	5.6	26
60	Optoelectronic Properties of Single-Crystalline Zn ₂ GeO ₄ Nanowires. Journal of Physical Chemistry C, 2014, 118, 8194-8199.	3.1	26
61	Opto-electrical properties of Sb-doped p-type ZnO nanowires. Applied Physics Letters, 2014, 104, .	3.3	25
62	Heterogeneous and Homogeneous Nucleation of Epitaxial NiSi ₂ in [110] Si Nanowires. Journal of Physical Chemistry C, 2011, 115, 397-401.	3.1	24
63	Transparent Antiradiative Ferroelectric Heterostructure Based on Flexible Oxide Heteroepitaxy. ACS Applied Materials & Interfaces, 2018, 10, 30574-30580.	8.0	24
64	The Influence of Surface Oxide on the Growth of Metal/Semiconductor Nanowires. Nano Letters, 2011, 11, 2753-2758.	9.1	23
65	In Situ Observation of Dehydration-Induced Phase Transformation from Na ₂ Nb ₂ O ₆ –H ₂ O to NaNbO ₃ . Journal of Physical Chemistry C, 2012, 116, 22261-22265.	3.1	23
66	Low Resistivity Metal Silicide Nanowires with Extraordinarily High Aspect Ratio for Future Nanoelectronic Devices. ACS Nano, 2011, 5, 9202-9207.	14.6	22
67	Single-crystalline δ-Ni2Si nanowires with excellent physical properties. Nanoscale Research Letters, 2013, 8, 290.	5.7	22
68	In Situ Observation of Au Nanostructure Evolution in Liquid Cell TEM. Journal of Physical Chemistry C, 2017, 121, 26069-26075.	3.1	22
69	The different roles of contact materials between oxidation interlayer and doping effect for high performance ZnO thin film transistors. Applied Physics Letters, 2015, 106, 051607.	3.3	21
70	Observing the evolution of graphene layers at high current density. Nano Research, 2016, 9, 3663-3670.	10.4	21
71	Flexible Heteroepitaxy Photoelectrode for Photo-electrochemical Water Splitting. ACS Applied Energy Materials, 2018, 1, 3900-3907.	5.1	21
72	Single-crystalline CuO nanowires for resistive random access memory applications. Applied Physics Letters, 2015, 106, .	3.3	19

#	Article	IF	CITATIONS
73	Atomic Visualization of the Phase Transition in Highly Strained BiFeO3 Thin Films with Excellent Pyroelectric Response. Nano Energy, 2015, 17, 72-81.	16.0	19
74	Nickel/Platinum Dual Silicide Axial Nanowire Heterostructures with Excellent Photosensor Applications. Nano Letters, 2016, 16, 1086-1091.	9.1	19
75	Applications of p-n homojunction ZnO nanowires to one-diode one-memristor RRAM arrays. Scripta Materialia, 2020, 187, 439-444.	5.2	19
76	Structural Analysis and Performance in a Dualâ€Mechanism Conductive Filament Memristor. Advanced Electronic Materials, 2021, 7, 2100605.	5.1	19
77	Growth of single-crystalline cobalt silicide nanowires with excellent physical properties. Journal of Applied Physics, 2011, 110, .	2.5	18
78	Self-formed conductive nanofilaments in (Bi, Mn)O for ultralow-power memory devices. Nano Energy, 2015, 13, 283-290.	16.0	17
79	Dynamic observation of reversible lithium storage phenomena in hybrid supercapacitor devices. Nano Energy, 2017, 41, 494-500.	16.0	17
80	<i>In situ</i> TEM observation of Au–Cu ₂ O core–shell growth in liquids. Nanoscale, 2019, 11, 10486-10492.	5.6	17
81	Bioinspired Engineering of a Bacteriumâ€Like Metal–Organic Framework for Cancer Immunotherapy. Advanced Functional Materials, 2020, 30, 2003764.	14.9	17
82	Pollen-Mimetic Metal–Organic Frameworks with Tunable Spike-Like Nanostructures That Promote Cell Interactions to Improve Antigen-Specific Humoral Immunity. ACS Nano, 2021, 15, 7596-7607.	14.6	17
83	Optimization of the nanotwin-induced zigzag surface of copper by electromigration. Nanoscale, 2016, 8, 2584-2588.	5.6	16
84	<i>In Situ</i> Investigation of Defect-Free Copper Nanowire Growth. Nano Letters, 2018, 18, 778-784.	9.1	15
85	Stability of nanoscale twins in copper under electric current stressing. Journal of Applied Physics, 2010, 108, 066103.	2.5	14
86	Low Interface Trap Densities and Enhanced Performance of AlGaN/GaN MOS High- Electron Mobility Transistors Using Thermal Oxidized Y ₂ 0 ₃ Interlayer. IEEE Electron Device Letters, 2015, 36, 1284-1286.	3.9	14
87	Mass transport phenomena in copper nanowires at high current density. Nano Research, 2016, 9, 1071-1078.	10.4	14
88	<i>In situ</i> TEM investigation of electron beam-induced ultrafast chemical lithiation for charging. Journal of Materials Chemistry A, 2020, 8, 648-655.	10.3	13
89	Cobalt silicide nanocables grown on Co films: synthesis and physical properties. Nanotechnology, 2010, 21, 485602.	2.6	12
90	Ni/NiO/HfO ₂ Core/Multishell Nanowire ReRAM Devices with Excellent Resistive Switching Properties. Advanced Electronic Materials, 2018, 4, 1800256.	5.1	12

#	Article	IF	CITATIONS
91	Atomic-Scale Localized Thinning and Reconstruction of Two-Dimensional WS ₂ Layers through <i>In Situ</i> Transmission Electron Microscopy/Scanning Transmission Electron Microscopy. Journal of Physical Chemistry C, 2020, 124, 14935-14940.	3.1	12
92	Atomic-scale investigation of Na3V2(PO4)3 formation process in chemical infiltration via in situ transmission electron microscope for solid-state sodium batteries. Nano Energy, 2021, 87, 106144.	16.0	12
93	Single-crystalline Ge nanowires and Cu3Ge/Ge nano-heterostructures. CrystEngComm, 2012, 14, 4570.	2.6	11
94	Observing phase transformation in CVD-grown MoS ₂ <i>via</i> atomic resolution TEM. Chemical Communications, 2018, 54, 9941-9944.	4.1	11
95	Direct Observation of Sublimation Behaviors in One-Dimensional In2Se3/In2O3 Nanoheterostructures. Analytical Chemistry, 2015, 87, 5584-5588.	6.5	10
96	Surface defect engineering: gigantic enhancement in the optical and gas detection ability of metal oxide sensor. RSC Advances, 2016, 6, 65146-65151.	3.6	10
97	In Situ TEM Investigation of the Electrochemical Behavior in CNTs/MnO ₂ -Based Energy Storage Devices. Analytical Chemistry, 2017, 89, 9671-9675.	6.5	10
98	Carbon Nanotube/Nitrogen-Doped Reduced Graphene Oxide Nanocomposites and Their Application in Supercapacitors. Journal of Nanoscience and Nanotechnology, 2017, 17, 5366-5373.	0.9	10
99	Phase Variations and Layer Epitaxy of 2D PdSe ₂ Grown on 2D Monolayers by Direct Selenization of Molecular Pd Precursors. ACS Nano, 2020, 14, 11677-11690.	14.6	10
100	Mimic Drug Dosage Modulation for Neuroplasticity Based on Chargeâ€Trap Layered Electronics. Advanced Functional Materials, 2021, 31, 2005182.	14.9	10
101	Atomic-scale silicidation of low resistivity Ni-Si system through in-situ TEM investigation. Applied Surface Science, 2021, 538, 148129.	6.1	10
102	Growth and properties of single-crystalline Ge nanowires and germanide/Ge nano-heterostructures. CrystEngComm, 2012, 14, 53-58.	2.6	9
103	Dynamic observation on the growth behaviors in manganese silicide/silicon nanowire heterostructures. Nanoscale, 2015, 7, 1776-1781.	5.6	9
104	Electron Beam Irradiation-Induced Deoxidation and Atomic Flattening on the Copper Surface. ACS Applied Materials & Interfaces, 2019, 11, 40909-40915.	8.0	9
105	In Situ Analysis of Growth Behaviors of Cu ₂ O Nanocubes in Liquid Cell Transmission Electron Microscopy. Analytical Chemistry, 2019, 91, 9665-9672.	6.5	9
106	Controlled growth of the silicide nanostructures on Si bicrystal nanotemplate at a precision of a few nanometres. CrystEngComm, 2011, 13, 3967.	2.6	8
107	A solid-state cation exchange reaction to form multiple metal oxide heterostructure nanowires. Nanoscale, 2016, 8, 17039-17043.	5.6	8
108	Observing Solid-State Formation of Oriented Porous Functional Oxide Nanowire Heterostructures by <i>in Situ</i> TEM. Nano Letters, 2018, 18, 6064-6070.	9.1	8

#	Article	IF	CITATIONS
109	Observing Growth and Crystallization of Au@ZnO Core–Shell Nanoparticles by <i>In Situ</i> Liquid Cell Transmission Electron Microscopy: Implications for Photocatalysis and Gas-Sensing Applications. ACS Applied Nano Materials, 2021, 4, 612-620.	5.0	8
110	Electronic Interactions and Charge-Transfer Dynamics for a Series of Yolk–Shell Nanocrystals: Implications for Photocatalysis. ACS Applied Nano Materials, 2022, 5, 8404-8416.	5.0	8
111	Atomic Imaging of Molybdenum Oxide Nanowires with Unique and Complex Periodicity by Advanced Electron Microscopy. Nano Letters, 2020, 20, 1510-1516.	9.1	7
112	Real Time Observation of the Formation of Hollow Nanostructures through Solid State Reactions. Analytical Chemistry, 2014, 86, 4348-4353.	6.5	6
113	Metal silicide nanowires. Japanese Journal of Applied Physics, 2015, 54, 07JA04.	1.5	6
114	Fabrication of (111)-Oriented Nanotwinned Au Films for Au-to-Au Direct Bonding. Materials, 2018, 11, 2287.	2.9	6
115	Dynamic observation on the functional metal oxide conversion behaviors in Fe3O4/ZnO heterostructures. Scripta Materialia, 2020, 177, 192-197.	5.2	6
116	Core-Shell Pd ₉ Ru@Pt on Functionalized Graphene for Methanol Electrooxidation. Journal of the Electrochemical Society, 2018, 165, H365-H373.	2.9	5
117	In situatomic-scale observation of the conversion behavior in a Cu-Zn alloy for twinnability enhancement. Applied Surface Science, 2022, 573, 151602.	6.1	5
118	In Situ Atomicâ€Scale Observation of Monolayer MoS ₂ Devices under Highâ€Voltage Biasing via Transmission Electron Microscopy. Small, 2022, 18, e2106411.	10.0	5
119	Metal Silicide Nanowires. ECS Transactions, 2007, 11, 3-6.	0.5	4
120	Shape control of nickel silicide nanocrystals on stress-modified surface. CrystEngComm, 2014, 16, 1611.	2.6	4
121	Solidâ€State Diffusional Behaviors of Functional Metal Oxides at Atomic Scale. Small, 2018, 14, 1702877.	10.0	4
122	Ultra-high annealing twin density in <211>-oriented Cu films. Scripta Materialia, 2020, 184, 46-51.	5.2	4
123	In-situ Transmission Electron Microscope Investigation of Atomic-scale Titanium Silicide Monolayer Superlattice. Scripta Materialia, 2021, 193, 6-11.	5.2	4
124	In situ atomic-scale TEM observation of Ag nanoparticle-mediated coalescence in liquids. Applied Surface Science, 2021, 546, 149057.	6.1	4
125	In situ manipulation of E-beam irradiation-induced nanopore formation on molybdenum oxide nanowires. Applied Surface Science, 2021, 544, 148874.	6.1	4
126	Observing resistive switching behaviors in single Ta2O5 nanotube-based memristive devices. Materials Today Nano, 2022, 18, 100212.	4.6	4

#	Article	IF	CITATIONS
127	Investigation and Effects of Wafer Bow in 3D Integration Bonding Schemes. Journal of Electronic Materials, 2010, 39, 2605-2610.	2.2	3
128	A Strategy to Synthesize Ultrahigh-N-Doped Hierarchical Carbons via Induced Î ² -Sheet from Silk Fibroin by <i>In Situ</i> Electrogelation/Electropolymerization. ACS Applied Energy Materials, 2020, 3, 3596-3608.	5.1	3
129	In situ TEM investigation of indium oxide/titanium oxide nanowire heterostructures growth through solid state reactions. Materials Characterization, 2022, 187, 111832.	4.4	3
130	Improved Performance of ZnO-Based Resistive Memory by Internal Diffusion of Ag Atoms. Journal of Nanoscience and Nanotechnology, 2012, 12, 6271-6275.	0.9	2
131	A Triode Device with a Gate Controllable Schottky Barrier: Germanium Nanowire Transistors and Their Applications. Small, 2019, 15, 1900865.	10.0	2
132	Unique amorphization-mediated growth to form heterostructured silicide nanowires by solid-state reactions. Materials and Design, 2019, 169, 107674.	7.0	2
133	In-situ transmission electron microscopy study of nanotwinned copper under electromigration. , 2010, , .		1
134	Synthesis of single-crystalline Ge ₁ Sb ₂ Te ₄ nanoplates in solution phase. CrystEngComm, 2016, 18, 2244-2246.	2.6	1
135	Enhancement in the Detection Ability of Metal Oxide Sensors Using Defectâ€Rich Polycrystalline Nanofiber Devices. Global Challenges, 2020, 4, 2000041.	3.6	1
136	Dynamic Observation of Electromigration in High Density Electroplated Nanotwinned Copper through in-Situ TEM. ECS Transactions, 2020, 97, 145-148.	0.5	1
137	In Situ Atomic‣cale Observation of Monolayer MoS ₂ Devices under Highâ€Voltage Biasing via Transmission Electron Microscopy (Small 7/2022). Small, 2022, 18, .	10.0	1
138	In-situ Microscopic Study of Cu Intragranular Electromigration. Materials Research Society Symposia Proceedings, 2005, 907, 1.	0.1	0
139	Effects of Strain Field of Si Bicrystal on the Formation of Nanoscale Silicides. ECS Transactions, 2007, 11, 83-88.	0.5	0
140	Multiple Heterostructures of Ni2Si/Si Formed by the Point Contact Reaction. ECS Transactions, 2009, 25, 41-44.	0.5	0
141	The operating mechanism of Schottky-gate nanosensors. , 2011, , .		0
142	Investigation of Indium Oxide Nanowire Transform to Indium Zinc Oxide (IZO) Via Solid State Reactions. ECS Transactions, 2020, 97, 105-108.	0.5	0
143	Fewâ€Layer MoS ₂ : Atomicâ€Scale Fabrication of Inâ€Plane Heterojunctions of Fewâ€Layer MoS ₂ via In Situ Scanning Transmission Electron Microscopy (Small 3/2020). Small, 2020, 16, 2070015.	10.0	0
144	Single Crystalline CuO Nanowire for Resistive Random Access Memory Application. ECS Meeting Abstracts, 2014, , .	0.0	0

#	ARTICLE	IF	CITATIONS
145	A Novel Three-Dimensional High Density Vertical Rram Arrays with Reduced Leakage Current. ECS Meeting Abstracts, 2020, MA2020-01, 1298-1298.	0.0	Ο
146	Revealing Resistive Switching Mechanism in <scp> CaFeO _x </scp> Perovskite System with <scp>Electroformingâ€Free</scp> and Reset <scp>Voltage ontrolled</scp> Multilevel Resistance Characteristics. Energy and Environmental Materials, 0, , .	12.8	0